Our ultraviolet Sun*

Bhola N. Dwivedi

High-resolution ultraviolet observations of the Sun from SOHO and TRACE spacecraft have provided a wealth of new information on plasma temperature, density, abundance anomaly, plasma flows, turbulence, wave motions, etc. in various solar structures. We present our ultraviolet Sun that has provided some landmark new results, especially from the line-shifts and broadenings of vacuum ultraviolet spectral lines, pinpointing the physical processes that maintain the Sun's hot corona, and accelerate the fast solar wind as well as locate its source region.

Keywords: Solar wind, solar corona, ultraviolet Sun.

THE Sun, with its surface temperature of 6000 K, was never expected to support an extended outer atmosphere or produce ultraviolet (UV) and X-rays. So, the discovery of the UV Sun was intriguing, dating back to 1801 with Ritter's observation of the decomposition of silver chloride on the short-wavelength side of the Sun's visible spectrum. Young and Harkness studied the corona spectroscopically during a total eclipse in 1869 and found a bright emission line at 530.3 nm (now known as the 'green' line, which could not then be identified and was ascribed to some unknown element called 'coronium'). In 1938, Hulburt[1] concluded that 'ultraviolet light, X-rays or particles of zero average charge' must be responsible for the E-layer of the Earth's ionosphere. Although this theory was highly speculative, it had the support of the work by Grotrian[2], who drew attention to the smearing-out of the Fraunhofer lines after scattering by coronal electrons. The 'coronium' puzzle was finally cracked down seventy years later by Bengt Edlén[3] in the 1940s, with his discovery that the 'green' coronal line was in fact due to iron with 13 of its electrons stripped-off. Such a situation was only possible if the plasma environment was million degrees hot. The 'green' and 'red' coronal lines are forbidden lines in the spectra of Fe XIV and Fe X respectively. At this point of time, the study of solar UV and X-rays became obviously worthwhile, but its implementation had to await the availability of vehicles to carry instruments above the absorbing layers of the Earth's atmosphere. The ultraviolet emission that the corona is hot enough to produce was first detected on 10 October 1946 with instruments built by Tousey and his colleagues at the US Naval Research Laboratory using captured German military V2 rockets[4]. The X-ray Sun was first discovered by Burnight[5] in 1949 using a rocket-borne pinhole camera. Since then, there has been a tremendous progress in the solar UV and X-ray observations and underlying physical processes in the Sun's million-degree hot atmosphere.

Observations from solar spacecraft in the 1960s and 1970s added much to our knowledge of the Sun's atmosphere; especially the manned NASA *Skylab* mission of 1973–74. UV and X-ray telescopes on-board gave the first high-resolution images of the chromosphere and corona, and the intermediate transition region. Images of active regions revealed a complex of loops which varied greatly over their lifetimes, while UV images of the quiet Sun showed that the transition region and chromosphere followed the 'network' character previously known from the Ca II K-line images. While we do not see surface details on any other star, we can resolve regions on the Sun as small as 150 km across, the size of a large city, using latest ground-based instruments, and 700 km with spacecraft instrumentation, though recognizing it is likely to be even better soon[6]. Figure 1 illustrates the magnetic network and prominences in the emission line of ionized helium at 30.4 nm, which is formed at about 60,000 to 80,000 K. For comprehensive reviews on topics from the Sun's interior to its exterior, including the solar wind and the solar observing facilities, the reader is referred to Dwivedi[7].

The ESA–NASA Solar and Heliospheric Observatory (SOHO) was launched on 2 December 1995 into an orbit about the inner Lagrangian (L1) point situated some 1.5×10^6 km from the Earth on the sunward side. Its twelve instruments, therefore, get an uninterrupted view of the Sun[8]. There are several imaging instruments, sensitive from visible-light wavelengths to the extreme-UV (EUV). The EIT, for instance, uses normal incidence optics to get full-Sun images several times a day in the wavelengths of lines emitted by the coronal ions Fe IX, Fe X, Fe XII, Fe XV (emitted in the temperature range 6×10^5 to 2.5×10^6 K) as well as the chromospheric He II 30.4 nm line. The CDS and SUMER are two spectrometers operating in the EUV region, capable of deducing temperatures, densities and other information from spectral line ratios. The UVCS

*Based on talks given at IIT, Kanpur on 25 January 2006, Homi Bhabha Centre for Science Education, Mumbai on 7 April 2006, and Vasanta College, Varanasi on 17 April 2006.

Bhola N. Dwivedi is in the Department of Applied Physics, Institute of Technology, Banaras Hindu University, Varanasi 221 005, India.
e-mail: bholadwivedi@yahoo.com

has been making spectroscopic observations of the extended corona from 1.25 to 10 solar radii from the Sun's centre, determining empirical values for densities, velocity distributions and outflow velocities of hydrogen, electrons and several minor ions.

The Transition Region and Coronal Explorer (TRACE)[9] satellite went into a polar orbit around the Earth in 1998. The spatial resolution is of order 1″ (725 km), and there are wavelength bands covering the Fe IX, Fe XII, and Fe XV lines as well as the *Ly-alpha* line at 121.6 nm. Its UV telescope has obtained images containing tremendous amount of small and varying features, for instance, active region loops are revealed to be only a few hundred kilometres wide, almost thread-like compared with their huge lengths. Their constant flickering and jouncing hint at the corona's heating mechanism. There is a clear relation of these loops and the larger arches of the general corona to the magnetic field measured in the photospheric layer. The crucial role of this magnetic field has only been realized in the past decade. The fields govern the transport of energy between the surface of the Sun and the corona. The loops, arches and holes appear to trace out the Sun's magnetic field (Figure 2 *a*, *b*). The latest in the fleet of spacecraft dedicated to viewing the Sun is the Reuven Ramaty High Energy Solar Spectroscopic Imager (RHESSI)[10], launched in 2002, which is providing images and spectra in hard X-rays (wavelengths less than about 4 nm). RHESSI's observations of tiny microflares may provide clues to the coronal heating mechanism.

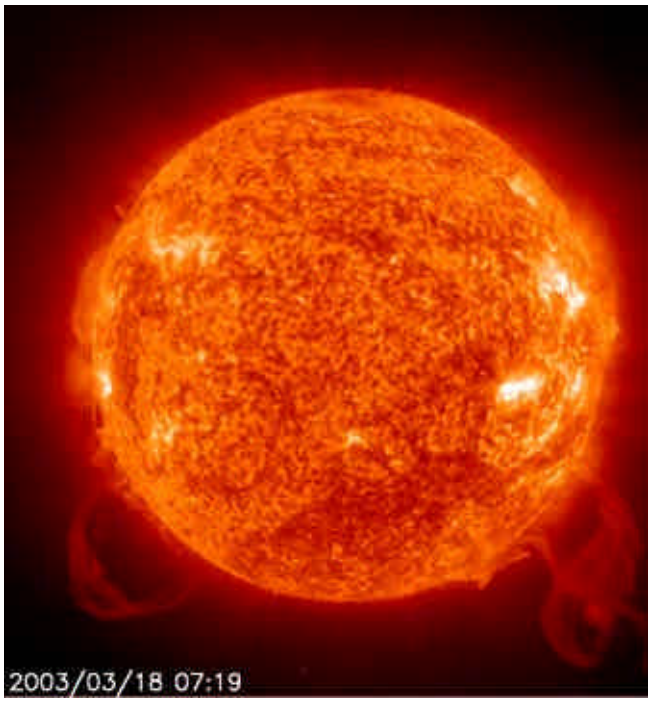

Figure 1. Magnetic network and prominences in the He II emission line at a wavelength of 30.4 nm, formed at about 60,000 to 80,000 K. This shows relatively cool material in the lower corona. Prominences are often seen at the origin of coronal mass ejections. The network is believed to be the site for wave generation (credit : EIT/SOHO).

Diagnostics of UV emission lines

The Sun's EUV and UV spectra, in the wavelength range from 46.5 to 161.0 nm (465 to 1610 Å), which is the spectral range of the SUMER spectrograph, provide unique opportunities for probing the solar atmosphere from the chromosphere to the corona (Figure 3; from Curdt *et al.*[11]). Emission line intensities and their ratios and line shapes are used to obtain diagnostic information on plasmas in the temperature range from 10^4 to more than 10^6 K, such as temperature, density, abundance, turbulence and flows. A full description of SUMER spectrograph and its performance is available in ref 12–15. Without a knowledge of the densities, temperatures and elemental abundances of space plasmas, almost nothing can be said regarding the generation and transport of mass, momentum and energy. Thus, since early in the era of space-borne spectroscopy, we have faced the task of inferring these plasma parameters for hot solar and other astrophysical plasmas from optically

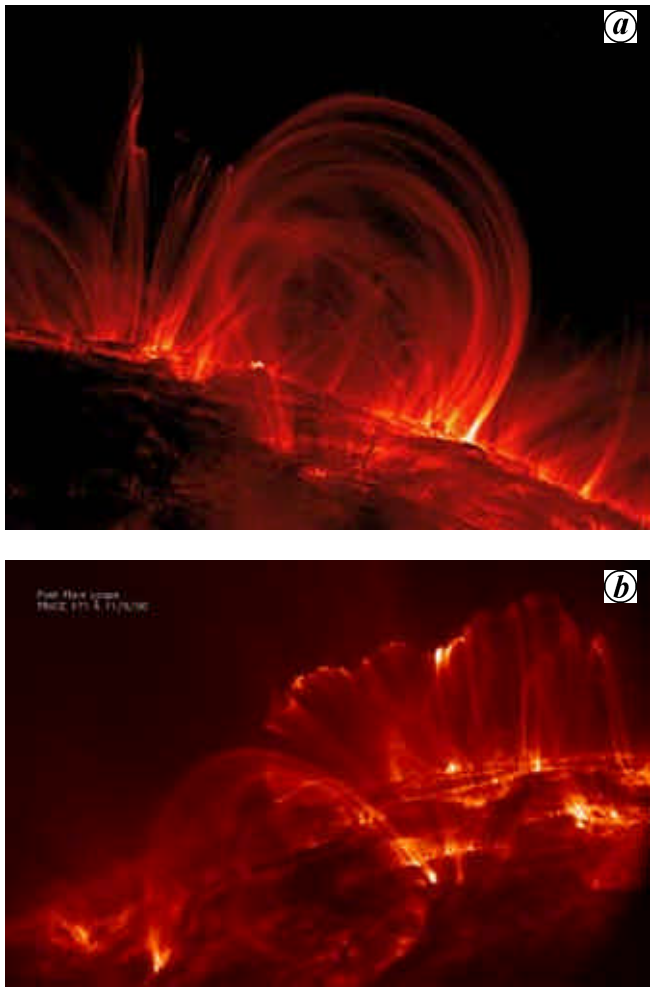

Figure 2. ***a***, Coronal loops, observed in the ultraviolet radiation Fe IX 17.1 nm (171 Å) by the TRACE spacecraft on 6 November 1999, extending 120,000 km off the Sun's surface ***b***, Post-flare loops, observed in the ultraviolet radiation Fe IX 17.1 nm (171 Å) by the TRACE spacecraft on 9 November 2000 (Credit: TRACE/NASA).

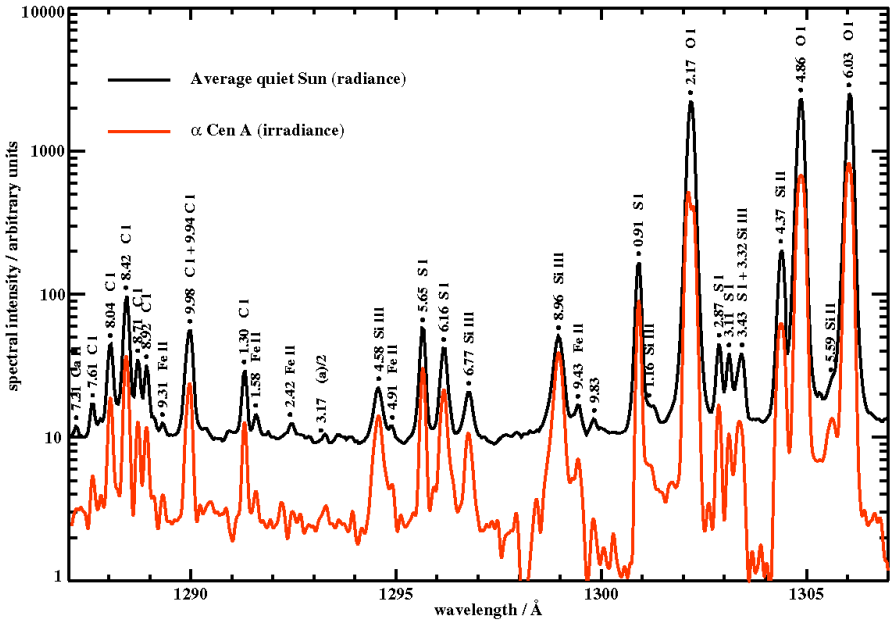

Figure 3. A close-up of a tiny part of the spectral atlas released from the SUMER instrument, compared with the irradiance spectrum of Alpha Cen A from HST–STIS. With the release of a new 'spectral atlas' from the SUMER instrument on-board SOHO, the world's astronomers have a much more complete roadmap of what could be described as the 'solar genome'. Also likened with its 'fingerprint', a star's full spectrum uniquely pins down all its defining characteristics: mass, elemental composition, age and rotational speed. The SUMER spectral atlas is the best-ever analysis of UV light from the Sun, spanning wavelengths from 67.0 to 160.9 nm (670 to 1609 Å), and identifies some 1100 distinct emission lines, of which more than 150 had not been recorded or identified before SOHO (credit: SUMER/SOHO, ESA–NASA; HST–STIS, NASA–ESA; Curdt *et al.*[11]).

thin emission-line spectra[15–19]. Spectroscopic diagnostics of the temperature and density structures of hot, optically thin plasmas using emission-line intensities is usually described in two ways. The simplest approach, the line-ratio diagnostics, uses an observed line-intensity ratio to determine density or temperature from theoretical density or temperature-sensitive line-ratio curves, based on an atomic model and taking account of physical processes for the line formation.

Prior to the SOHO mission, there was little information available on the density and temperature structure in coronal holes. Data from *Skylab* were limited, due to the very low intensities in holes and poor spectral resolution, leading to many line blends. High-resolution UV observations from instruments on SOHO spacecraft provided the opportunity to infer the density and temperature profile in coronal holes[20]. Comparing the electron temperatures with ion temperatures, it was concluded that ions are extremely hot and the electrons are relatively cool. Using the CDS and SUMER instruments on the SOHO spacecraft, electron temperatures were measured as a function of height above the limb in a coronal hole. Observations of two lines from the same ion, O VI 103.2 nm (1032 Å) from SUMER and O VI 17.3 nm (173 Å) from CDS, were made to determine temperature gradient in a coronal hole[21]. In this manner, temperature of around 0.8 MK close to the limb was deduced, rising to a maximum of less than 1 MK at 1.15 $R_{\odot}$, then falling to around 0.4 MK at 1.3 $R_{\odot}$. These observations preclude the existence of temperatures much over 1 MK at any height near the centre of a coronal hole. Wind acceleration by temperature effects is, therefore, inadequate as an explanation of the high-speed solar wind and it becomes essential to look for other effects, involving the momentum and the energy of Alfvén waves.

Recently, we investigated the potential for plasma diagnostics of forbidden transitions from ground levels in nitrogen-like ions[22]. We have shown several line-intensity ratios, which can be effectively used for density diagnostics in the solar corona. Some of the lines have been measured by SUMER for the first time. We investigated the effects of photospheric radiation, proton collisional excitations, additional configurations and resonances on level populations, in order to assess the importance of these processes in the calculation of line emissivities. We compared the line ratios with observations from SUMER on quiet-Sun and active regions, and measured the electron density and temperature of the emitting plasma. We showed that in a few cases current atomic data are still not able to reproduce the observations and that further work is required to solve inconsistencies between observations and theoretical predictions. We have also investigated First Ionization Potential (FIP) effect measurements in the off-limb corona[23,24]. We found that Mg/Ne relative abundance is highly variable in the complex, cool core of the active region, strongly correlated with line intensity and magnetic structures. Mg abun-

dance enhancements relative to Ne reach up to a factor of 8.8. In off-limb active region plasma, the FIP bias inside elements' class is dependent on the FIP value, being higher for the very low-FIP element K. The FIP bias versus FIP problem is still open.

Line shifts and broadenings give information about the dynamic nature of the solar and stellar atmospheres. The transition region spectra from the solar atmosphere are characterized by broadened line profiles. The nature of this excess broadening puts constraints on possible heating processes. Systematic red shifts in transition-region lines have been observed in both solar and stellar spectra of late-type stars. On the Sun, outflows of coronal material have been correlated with coronal holes. Excess broadening of coronal lines above the limb provides information on wave propagation in the solar wind. Striking difference in the width of line profiles observed on disk and in a polar coronal hole (Figure 4) led to the discovery of the large velocity anisotropy, and solar wind acceleration by ion-cyclotron resonance[25]. An intriguing observation with the UVCS has shown that particular ions, specifically highly ionized oxygen atoms, have temperatures in coronal holes, some 100 MK of kinetic temperature, that are much higher than those characterized by electrons and protons making up the bulk of the plasma[25]. There seems to be some directionality to the oxygen temperatures – they are higher, perpendicular to the magnetic field lines than parallel to them, a result that is in agreement with interplanetary spacecraft sampling the particles making up the solar wind. The observation seems to call for high-frequency ion-cyclotron waves[26] that are produced lower down in the atmosphere as low-frequency waves but which through some cascade process end up at the observed frequencies.

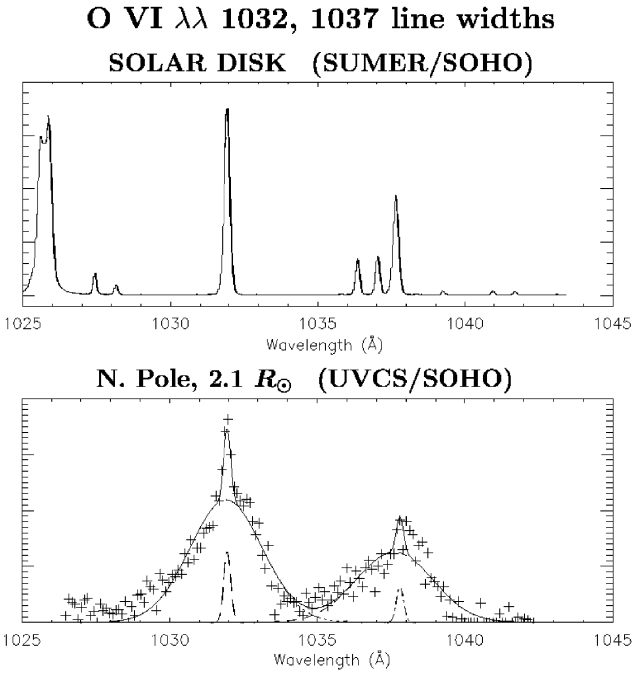

Figure 4. UVCS/SOHO observations of the O VI 103.2 nm (1032 Å) and 103.7 nm (1037 Å) line profiles at 2.1 solar radii, in a polar coronal hole (lower panel)[25]. Each line consists of the coronal profile and narrow contribution from stray light plus F corona, which are separately constrained. Data points are shown as crosses, coronal profiles by dashes, and total observed profile by a solid line. Widths of coronal emission lines tell us about the ion velocity distribution measured along the line of sight. These extremely broad O VI lines yield velocities up to 500 km s^{-1}, which corresponds to kinetic temperatures of 200 MK. For comparison, the SUMER/SOHO solar disk observations in the same range of spectrum (upper panel) are shown. The respective O VI 103.2 and 103.7 nm lines are much narrower, with widths of about 30 km s^{-1} (credit: UVCS, SUMER, ESA–NASA).

We can directly measure physical parameters such as electron density, temperature, flow speeds, etc. in the corona from emission-line diagnostics. However, we cannot directly measure coronal magnetic field strength, resistivity, viscosity, turbulence, waves, etc. New powerful tools of coronal seismology have enabled the detection of MHD waves by TRACE and EIT, spectroscopic measurements of line-widths by SUMER and CDS, ion and electron temperature anisotropy measurements with UVCS, and microflares by RHESSI. For a century, astronomers have measured the photospheric magnetic field using magnetographs, which observe the Zeeman effect. A spectral line can split into two or more lines with slightly different wavelengths, and polarizations in the presence of magnetic field. But the Zeeman effect observations for the corona have yet to be done. The spectral splitting is too small to be detected with the present instrumentation, so we have to resort to mathematical extrapolation from photospheric magnetic field. Figure 5 *a* shows the coronal magnetic field as obtained by force-free extrapolation from photospheric magnetograms[27]. The closed loops mostly correspond to bipolar active regions (Figure 5 *b*), or also may bridge widely separated regions of opposite polarity. The open field lines, however, illustrate the coronal magnetic field that is open to the heliosphere and correspond to the magnetic flux carried away by the solar wind.

Coronal holes and solar wind

Observations from the *Skylab* firmly established that the high-speed solar wind originates in coronal holes, which are well-defined regions of strongly-reduced UV and X-ray emissions[28]. More recent data from *Ulysses* showed the importance of the polar coronal holes, particularly at times near the solar minimum, when dipole field dominates the magnetic field configuration of the Sun. The mechanism for accelerating the wind to the high values observed, of the order of 800 km s^{-1}, is not yet fully understood. The Parker model is based on a thermally-driven wind. To reach such high velocities, temperatures of the order 3 to 4 MK would be required near the base of the corona. However, other processes are available for acceleration of the wind, for example, the direct transfer of momentum from MHD waves, with or without dissipation. This process

results from the decrease in momentum of the waves as they enter less dense regions, coupled with the need to conserve momentum of the total system. If this transfer predominates, it may not be necessary to invoke very high coronal temperatures at the base of the corona. That the solar wind is emanating from coronal holes (open magnetic field regions in the corona) has been widely accepted since the *Skylab* era. But there was little additional direct observational evidence to support this view. Hassler *et al.*[29] found the Ne VIII emission blue-shifted in the north polar coronal hole along the magnetic network boundary interfaces compared to the average quiet-Sun flow. These Ne VIII observations have revealed the first two-dimensional coronal images showing velocity structure in a coronal hole, and provided a strong evidence that coronal holes are indeed the source of the fast solar wind.

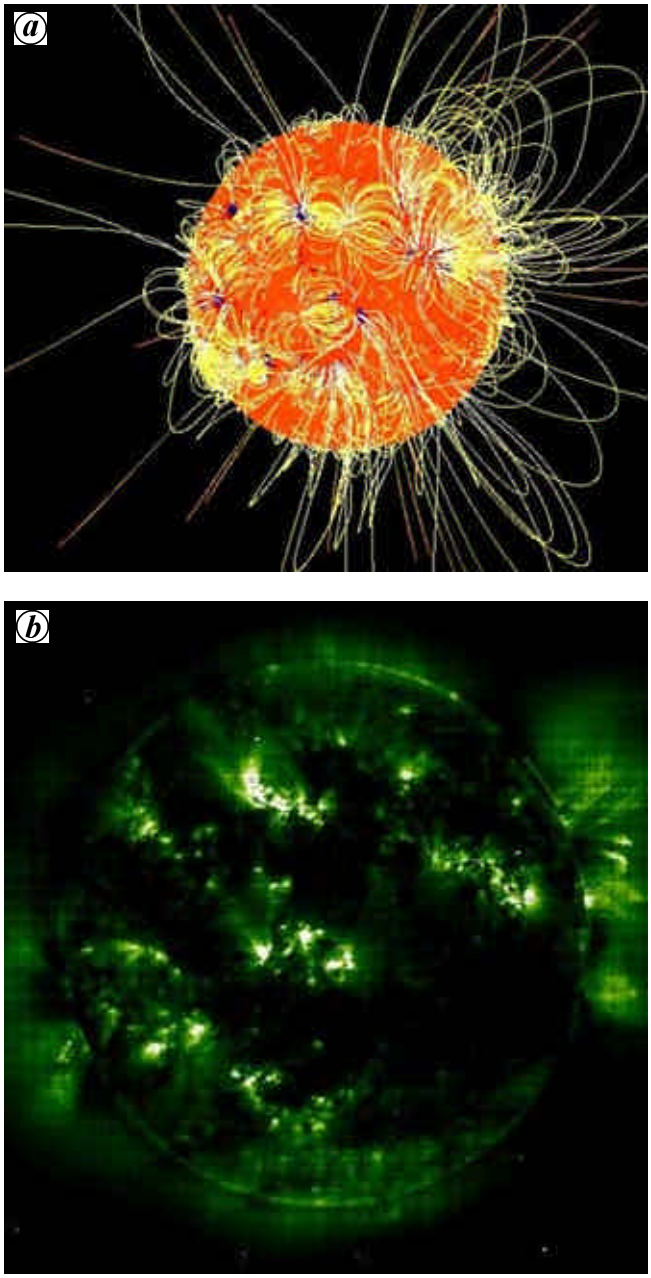

Figure 5. ***a***, Coronal magnetic field as obtained by force-free extrapolation from photospheric magnetograms[27]. Closed loops mostly correspond to bipolar active regions, or also may bridge widely separated regions of opposite polarity, whereas open field lines illustrate coronal magnetic field that is open to the heliosphere and corresponds to the magnetic flux carried away by the solar wind (credit: Wiegelman and Solanki[27]). ***b***, Active regions mainly consist of closed magnetic loops in which plasma is confined and causes bright emission. The large-scale magnetic field is open in coronal holes, from which plasma escapes on open field lines as solar wind, and where the line emission is strongly reduced (credit: EIT/SOHO).

Tu *et al.*[30] have now successfully identified the magnetic structures in the solar corona where the fast solar wind originates. Using images and Doppler maps from the SUMER spectrograph and magnetograms from the MDI instrument on the SOHO spacecraft, they have reported the solar wind flowing from funnel-shaped magnetic fields which are anchored in the lanes of the magnetic network near the surface of the Sun (Figure 6). This landmark research leads to a better understanding of the magnetic nature of the solar wind source region. The heavy ions in the coronal source regions emit radiation at certain UV wavelengths. When they flow towards the Earth, the wavelengths of the UV emission become shorter, which can be used to identify the beginning of the solar wind outflow.

Previously it was believed that the fast solar wind originates on any given open field line in the ionization layer of hydrogen atom, slightly above the photosphere. However, the low Doppler shift of an emission line from carbon ions shows that bulk outflow has not yet occurred at a height of 5000 km. The solar wind plasma is now considered to be supplied by plasma stemming from the many small magnetic loops, with only a few thousand kilometres in height, crowding the funnel. Through magnetic reconnection, the plasma is fed from all the sides to the funnel, where it may be accelerated and finally form the solar wind. The fast solar wind starts to flow out from the top of the funnels in coronal holes with a flow speed of about 10 km s^{-1}. This outflow is seen as large patches in Doppler blue shift (hatched areas in the Figure 6) of a spectral line emitted by Ne^{+7} ions at a temperature of 600,000 K, which can be used as a good tracer for the hot plasma flow. Through a comparison with the magnetic field, as extrapolated from the photosphere by means of the MDI magnetic data, it has been found that the blue-shift pattern of this line correlates best with the open field structures at 20,000 km.

Based on these investigations, a new model has been proposed to explain the origin of the fast solar wind[31], which is shown in Figure 7. The transition region in coronal holes consists of magnetic loops of sizes ~ 5 Mm or less. The legs of the loops keep moving due to supergranular convection, thereby transferring kinetic energy into magnetic energy that is stored in the loops. They may eventually collide with the funnel and reconnect with pre-existing open fields. Plasma in the loops is then released,

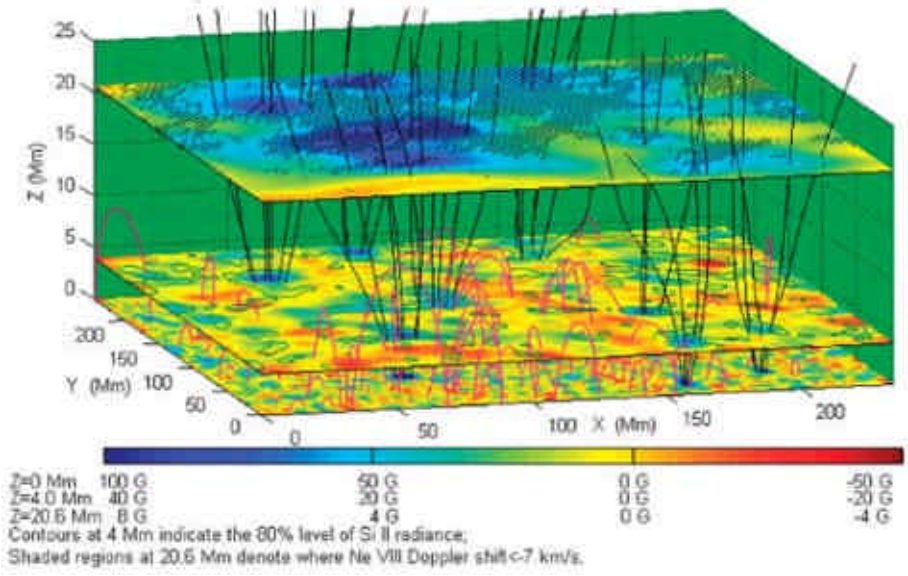

Figure 6. Source regions of the fast solar wind in magnetic funnels of a coronal hole. The magnetic field magnitude is shown in two planes at 4 and 20 Mm. Hatched areas indicate outflow speeds of neon ions larger than 7 km s^{-1}. Open field is indicated by black lines, and closed loops in magenta colour. They hardly reach a height of 10 Mm (from Tu *et al.*[30]).

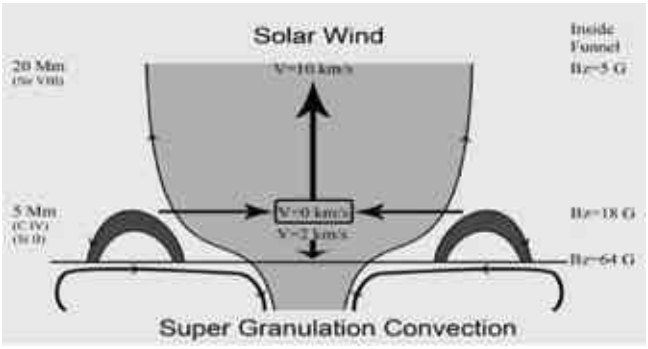

Figure 7. Source regions of the fast solar wind in a magnetic funnel of a coronal hole. This sketch illustrates the scenario of the solar wind origin and its energy and mass supply, mainly through side loops. Ultimately, convection is the driver of solar wind outflow in coronal funnels. Mass as well as wave energy are delivered to the funnel by magnetic reconnection. Funnel and loops are drawn according to their real scale sizes[31].

resulting in upflows and downflows. Parts of the plasma contained in reconnecting loops move into the corona. Supergranular motion drives the horizontal exchange of mass and energy between neighbouring flux tubes up to 5 Mm. Vertical transport becomes important above 5 Mm, where reconnection between field lines of funnels and loops ceases. This is where the radial acceleration of the solar wind starts.

Magnetic fields channel the transport of charged particles. Thus solar wind particles flow along invisible magnetic field lines, much like cars on a highway. When the magnetic field lines bend straight out into space (as in coronal hole regions), the solar wind acts like cars on a drag strip, racing along at high speed. When the magnetic field lines bend sharply back to the solar surface, like the pattern of iron filings around a bar magnet, the solar wind acts like cars in city traffic and emerges relatively slowly. This is well known for over three decades and is used to give a crude estimate for the speed of the solar wind – either fast or slow. In the new work by McIntosh and Leamon[32], the speed and composition of the solar wind emerging from a given area of the solar corona are estimated from the characteristics of the chromosphere underlying that piece of the corona. Using SOHO's EIT instrument as a 'finder', they isolated regions of the solar corona with open magnetic field lines (coronal holes) and closed fields (active regions). Then, using the earth-orbiting TRACE to measure the time sound waves took to travel between the heights of formation of two chromospheric continuua, they were able to demonstrate that sound travel time predicted not only solar wind speed measured by ACE, but its isotopic compositon as well.

Wave activity in the Sun's atmosphere

Hassler *et al.*[33] carried out a rocket-borne experiment to observe off-limb line width profile of MgX 60.9 nm (609 Å) and 62.5 nm (625 Å) and reported increasing line width with altitude (up to 70,000 km). This observation provided the first likely signature of outward propagating undamped Alfvén waves. SUMER and CDS spectrometers recorded several line profiles and reported the broadening of emission lines. These results are consistent with outward propagation of undamped Alfvén waves travelling through regions of

decreasing density[34]. However, Harrison *et al.*[35] reported the narrowing of the MgX 62.5 nm (625 Å) line with height in the quiet near-equatorial solar corona, and concluded that this narrowing is likely evidence of dissipation of Alfvén waves in closed field-line regions. Similarly, a significant change in slope of the line width as a function of height was seen in polar coronal holes by O'Shea *et al.*[36] at an altitude of ≈ 65 Mm. These results obtained with the CDS, if confirmed, could be crucial in understanding the coronal heating mechanisms. Due to the broad instrumental profile, the CDS instrument can only study line-width variations and cannot provide measurements of the line width itself, and, hence, of the effective ion temperature. The latter quantity is critical in constraining theoretical models of coronal heating and solar wind acceleration, for instance, through the dissipation of high-frequency waves generated by chromospheric reconnection. Wilhelm *et al.*[37] studied the problem further by analysing data recorded with the SUMER spectrograph in the MgX doublet together with other neighbouring lines in both the quiet equatorial corona and in a polar coronal hole. Due to the high spectral resolution of SUMER, they were able to obtain profiles of both MgX emission lines and measure their widths and variations as a function of height. Their work showed that line widths of both components of the MgX doublet measured by SUMER monotonically increase in the low corona in equatorial regions in altitude ranges for which scattered radiation from the disk does not play a major role. They did not find any evidence for a narrowing of the emission lines above 50 Mm. The same holds true for a coronal hole, but they could not exclude the possibility of a constant width above 80 Mm (Figure 8).

While there have been reports of emission-line broadening with altitude using SUMER, the CDS observations presented by Harrison *et al.*[35], already noted, appeared to show emission-line narrowing. In order to resolve the apparent discrepancies, a joint CDS/SUMER observational sequence was successfully executed during the SOHO/MEDOC campaign in November and December 2003. The joint measurements were performed near the east limb (Wilhelm *et al.*[38]). The pointing locations of the spectrometers are shown in Figure 9 *a* and *b*, superimposed on He II and Fe XII solar images taken by EIT. In the western corona, SUMER made additional exposures with a similar observational sequence from 13 : 02 to 15 : 06 UTC. Since the corona was very hot there, the slit positions are shown together with the Fe XII and Fe XV windows of EIT in Figure 9 *c* and *d*.

The relative widths of the spectral lines observed by SUMER are shown in Figure 10, separately for the eastern and western FOVs. In cases for which more than one observation was available, mean values have been shown. The range of v_1/e extends from 35 to 49 km s^{-1} in the relatively quiet eastern corona, and from 33 to 48 km s^{-1} in the active western corona. No significant differences could be noticed within the uncertainty margins. The MgX and CaX lines show slight increases with height in the east, but are rather constant in the west. The Fe XII line is a little narrower in the west. Of particular interest was that the lines of Ca XIII and Fe XVIII were seen in the west, where they could be compared with the Ca X and Fe XII lines along the same LOS. In the relatively quiet equatorial corona above a small prominence, Wilhelm *et al.*[38] found no or slight increase in the line widths of coronal emission lines with altitude from measurements both with CDS and SUMER. Taking the combined uncertainty margins into account, the relative variations for MgX were considered to be consistent, although the absolute widths could not be compared given the different instrumental spectral transfer functions. The SUMER observations in-

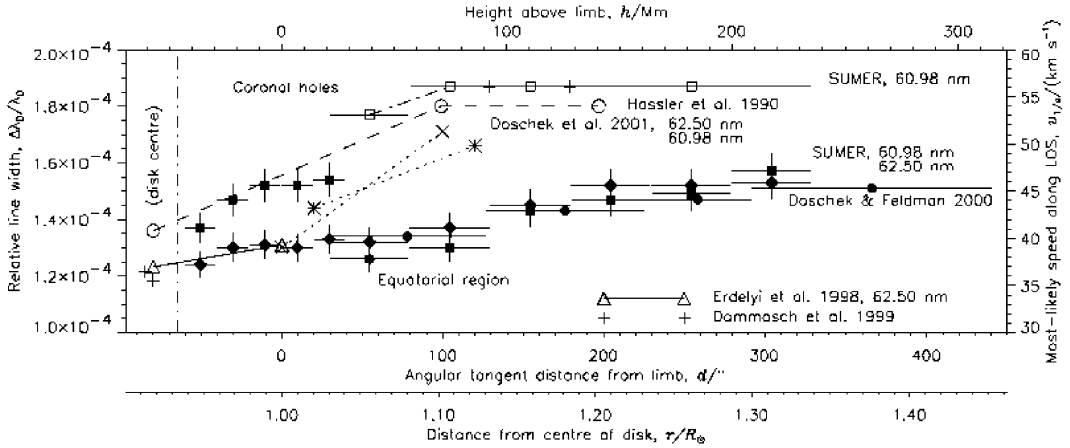

Figure 8. Relative line-width variations as a function of radial distance from the Sun. Literature data and results obtained in this work (annotated 'SUMER') are compiled for the Mg X doublet in equatorial and coronal-hole regions. A classification of the observations by Hassler *et al.*, of which only three typical values are shown, is not defined in their 1990 paper. Integration intervals and the SUMER uncertainty margins are marked by horizontal and vertical bars. Related data points are in some cases connected by lines of various styles. They are meant to improve the orientation of the reader, but not as physical interpolations, in particular, for those points representative of centre-of-disk values displayed here near –80″ (from Wilhelm *et al.*[37]).

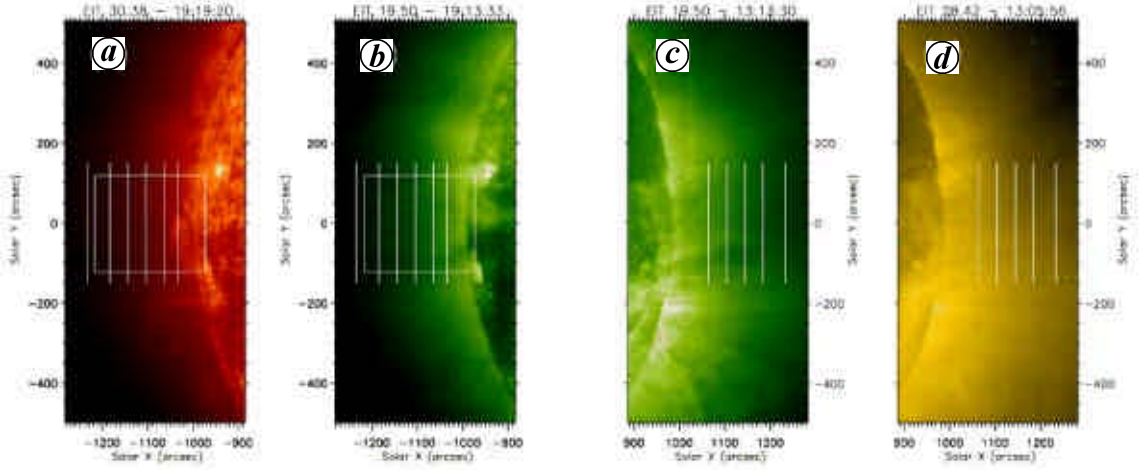

Figure 9. Positions of CDS FOVs (rectangles) and SUMER slit pointing locations in relation to He II, Fe XII and Fe XV solar images of 4 December 2003 (courtesy of the EIT consortium). Joint observations were obtained in the eastern corona. At low altitudes, a prominence caused a slight disturbance there. ***a***, He II spectral window; ***b***, Fe XII window near the east limb; ***c***, Fe XII window, and ***d***, Fe XV window near the west limb (from Wilhelm *et al.*[38]).

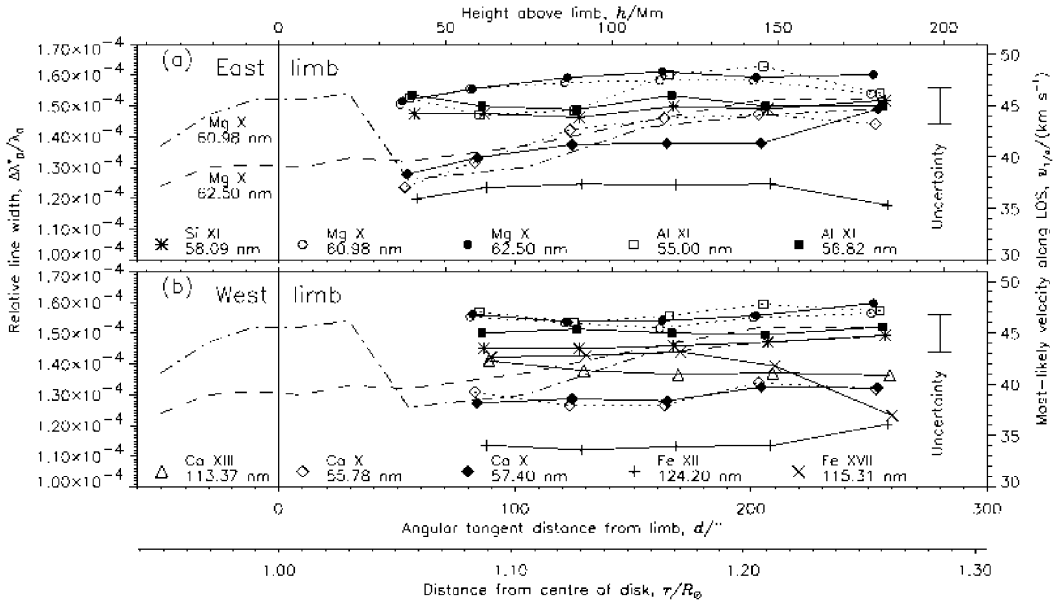

Figure 10. Summary of SUMER line-width measurements in terms of relative line width, $\Delta l_D^*/l_0$, of the various ions, as well as their most likely velocity along the LOS, n_1/e, as a function of distance from the limb. (***a***) Measurements above the east limb. ***b***, Measurements above west limb. Dashed and dash-dotted lines indicate the MgX observations of SUMER in November 1996. Increase in the width of the 60.98 nm line near the limb is caused by blends of O III and O IV transition-region lines. Near the centre of the solar disk a value of $\Delta l_D^*/l_0 \approx 1.2 \times 10^{-4}$ was observed for MgX. At each slit position, an altitude range of ≈10″ was covered. For the sake of clarity, the plot symbols of various spectral lines are spread over this range (from Wilhelm *et al.*[38]).

dicated even less line-width variations with height in the more active corona. Singh *et al.*[39] found height variations of line profiles in the visible light that depended on the formation temperatures of the lines. Thus, the solar conditions appear to have a direct influence on the line-width variations with height. Whether this dependence can account for the past apparent discrepancies cannot unambiguously be decided with the information available. More observations for different coronal activity levels are needed for this task. However, this joint study concluded that CDS and SUMER relative line-width measurements did not lead to inconsistencies if the same solar region is under study.

Dwivedi and Srivastava[40] have investigated the effect of viscosity and magnetic diffusivity on the spatial variation of damping length scales and energy flux density of high frequency Alfvén waves as a function of radial height. They have concluded a strong viscous and resistive damping of Alfvén waves in coronal holes. This result is in agreement with that of O'Shea *et al.*[41], who find a decrease in line widths above a radial height of about 1.23 $R_\odot$

and attribute it to a reduction in the non-thermal component of the line widths caused by a damping of upwardly propagating Alfvén waves.

Concluding remarks

Our UV Sun has provided a large amount of information concerning the physical processes taking place in the solar atmosphere from highly successful spacecraft SOHO, and TRACE. We have presented only a few of the significant results with regard to the tremendous progress made in pinpointing the processes that maintain the Sun's hot corona and accelerate the solar wind as well as its source region. And the quest to unravel the secrets of the Sun's mysteries goes on... .

1. Hulburt, E. O., Photoelectric ionization in the ionosphere. *Phys. Rev.*, 1938, **53**, 344–351.
2. Grotrian, W., Ergebnisse der Potsdamer Expedition zur Beobachtung der Sonnenfinsternis am 9. Mai 1929 in Takengon (Nordsumatra). 6. Mitteilung. Über die Intensitätsverteilung des kontinuierlichen Spektrums der inneren Korona. Mit 8 Abbildungen *Z. Astrophys.*, 1931, **3**, 199.
3. Edlén, B., Die deutung der emissionslinien in spektrum derSonnenkorona. *Z. Astrophys.*, 1943, **22**, 30–64.
4. Baum, W. A., Johnson, F. S., Oberly, J. J., Rockwood, C. C., Strain, C. V. and Tousey, R., Solar ultraviolet spectrum to 88 kilometers. *Phys. Rev.*, 1946, **70**, 781–782.
5. Burnight, T. R., Soft X-radiation in the upper atmosphere. *Phys. Rev.*, 1949, **76**, 165.
6. Dwivedi, B. N. (ed.), Dynamic Sun: an introduction. In *Dynamic Sun*, Cambridge University Press, Cambridge, 2003, pp. 1–7.
7. Dwivedi, B. N. (ed.), *Dynamic Sun*, Cambridge University Press, Cambridge, 2003.
8. Dwivedi, B. N. and Mohan, A., SOHO hunts elusive solar prey. *Curr. Sci.*, 1997, **72**, 437–440.
9. Handy, B. N. *et al.*, Calibrated H I Lyman alpha observations with TRACE. *Solar Phys*., 1999, **187**, 229–260.
10. Lin, R. P. *et al*., The Reuven High-Energy Solar Spectroscopic Imager (RHESSI). *Solar Phys*., 2002, **210**, 3–32.
11. Curdt, W., Brekke, P., Feldman, U., Wilhelm, K., Dwivedi, B. N., Schühle, U. and Lemaire, P., The SUMER spectral atlas of solar-disk features. *Astron. Astrophys*., 2001, **375**, 591–613.
12. Wilhelm, K. *et al*., SUMER – Solar ultraviolet measurements of emitted radiation. *Solar Phys*., 1995, **162**, 189–231.
13. Wilhelm, K. *et al*., First results of the SUMER telescope and spectrometer on SOHO – I. spectra and spectroradiometry. *Solar Phys*., 1997, **170**, 75–104.
14. Lemaire, P. *et al*., First results of the SUMER telescope and spectrometer on SOHO – II. Imagery and data management. *Solar Phys*., 1997, **170**, 105–122.
15. Wilhelm, K., Dwivedi, B. N., Marsch, E. and Feldman, U., Observations of the Sun at vacuum ultraviolet wavelengths from space. Part I: concepts and instrumentation. *Space Sci. Rev.*, 2004, **111**, 415–480.
16. Dwivedi, B. N., EUV spectroscopy as a plasma diagnostic. *Space Sci. Rev.*, 1994, **65**, 289–316.
17. Mason, H. E. and Monsignori-Fossi, B. C., Spectroscopic diagnostics in the VUV for solar and stellar plasmas. *Astron. Astrophys. Rev.*, 1994, **6**, 123–179.
18. Dwivedi, B. N., Mohan, A. and Wilhelm, K., Vacuum-ultraviolet emission line diagnostics for solar plasma. In *Dynamic Sun* (ed. Dwivedi, B. N.), Cambridge University Press, Cambridge, 2003, pp. 353–373.
19. Wilhelm, K., Dwivedi, B. N., Marsch, E. and Feldman, U., *Space Sci. Rev.*, 2006 (in preparation).
20. Wilhelm, K., Marsch, E., Dwivedi, B. N., Hassler, D. M., Lemaire, P., Gabriel, A. H. and Huber, M. C. E., The solar corona above polar coronal holes as seen by SUMER on SOHO. *Astrophys. J.*, 1998, **500**, 1023–1038.
21. David, C., Gabriel, A. H., Bely-Dubau, F., Fludra, A., Lemaire, P. and Wilhelm, K., Measurement of the electron temperature gradient in a solar coronal hole. *Astron. Astrophys*., 1998, **336**, L90–L94.
22. Mohan, A., Landi, E. and Dwivedi, B. N., On the EUV/UV plasma diagnostics for nitrogen-like ions from spectra obtained by SOHO/SUMER. *Astrophys. J.*, 2003, **582**, 1162–1171.
23. Dwivedi, B. N., Curdt, W. and Wilhelm, K., Analysis of EUV off-limb spectra obtained with SUMER/SOHO: Ne VI/Mg VI emission lines. *Astrophys. J.*, 1999, **517**, 516–525.
24. Dwivedi, B. N., Mohan, A. and Landi, E., FIP effect and FIP-dependent bias in the solar corona. In *Stars as Suns: Activity, Evolution and Planets* (eds Dupree, A. K. and Benz, A. O.), ASP Conf. Ser., 2004, vol. 219, pp. 493–497.
25. Kohl, J. L. *et al*., First results from the SOHO ultraviolet coronagraph spectrometer. *Solar Phys*., 1997, **175**, 613–644.
26. Tu, C.-Y., Marsch, W., Wilhelm, K. and Curdt, W., Ion temperatures in a solar polar coronal hole observed by SUMER on SOHO. *Astrophys. J.*, 1998, **503**, 475–488.
27. Wiegelmann, T. and Solanki, S. K., Why are coronal holes indistinguishable from the quiet Sun in transition region radiation? In Proc. The SOHO15 Workshop – Coronal Heating, ESA, SP-575, 2004, pp. 35–40.
28. Zirker, J. B. (ed.), *Coronal Holes and High Speed Solar Wind Streams*, Colorado Associated Univ. Press, Boulder, 1977.
29. Hassler, D. M. *et al*., Solar wind outflow and the chromospheric magnetic network. *Science*, 1999, **283**, 810–813.
30. Tu, C.-Y. *et al*., Solar wind origin in coronal funnels. *Science*, 2005, **308**, 519–523.
31. Tu, C.-Y. *et al*., The height of solar wind origin in coronal funnels and a 3-D scenario for solar wind formation. In *Solar Wind Eleven*, 2006 (in press).
32. McIntosh, S. W. and Leamon, R. J., Is there a chromospheric footprint of the solar wind?. *Astrophys. J.*, 2005, **624**, L117–L120.
33. Hassler, D. M., Rottman, G. J., Shoub, E. C. and Holzer, T. E., Line broadening of Mg X 609 and 625 A coronal emission lines observed above the solar limb. *Astrophys. J.*, 1990, **348**, L77–L80.
34. Erdélyi, R., Doyle, J. G., Perez, M. E. and Wilhelm, K., Center-to-limb line width measurements of solar chromospheric, transition region and coronal lines. *Astron. Astrophys*., 1998, **337**, 287–293.
35. Harrison, R. A., Hood, A. W. and Pike, C. D., Off-limb EUV line profiles and the search for wave activity in the low corona. *Astron. Astrophys*., 2003, **392**, 319–327.
36. O'Shea, E., Banerjee, D. and Poedts, S., Variation of coronal line widths on and off the disk. *Astron. Astrophys*., 2003, **400**, 1065–1070.
37. Wilhelm, K., Dwivedi, B. N. and Teriaca, L., On the widths of the Mg X lines near 60 nm in the corona. *Astron. Astrophys*., 2004, **415**, 1133–1139.
38. Wilhelm, K., Fludra, A., Teriaca, L., Harrison, R. A., Dwivedi, B. N. and Pike, C. D., The widths of vacuum-ultraviolet spectral lines in the equatorial solar corona observed with CDS and SUMER. *Astron. Astrophys.*, 2005, **435**, 733–741.
39. Singh, J., Ichimoto, K., Sakurai, T. and Muneer, S., Spectroscopic studies of the solar corona. IV. physical properties of coronal structure. *Astrophys. J*., 2003, **585**, 516–523.
40. Dwivedi, B. N. and Srivastava, A. K., On the propagation and dissipation of Alfvén waves in coronal holes. *Solar Phys.* 2006, **237**, 143–152.
41. O'Shea, E., Banerjee, D. and Doyle, J. G., On the widths and ratios of Mg X 609.79 and 624.94 Å lines in polar off-limb regions. *Astron. Astrophys*., 2005, **436**, L43–L46.

ACKNOWLEDGEMENTS. This work is supported by the Indian Space Research Organization under its RESPOND programme. I thank both the referees for their valuable comments.

Received 19 April 2006; revised accepted 5 July 2006